Journal of General Virology (2014), **95**, 2146–2154 **DOI** 10.1099/vir.0.064733-0

Characterization of Barmah Forest virus pathogenesis in a mouse model

Lara J. Herrero,[1,2]† Brett A. Lidbury,[3]†‡ Jayaram Bettadapura,[1,2] Peng Jian,[1,2] Belinda L. Herring,[1,4] William J. Hey-Cunningham,[4] Kuo-Ching Sheng,[1] Andrew Zakhary[2] and Suresh Mahalingam[1,2]

Correspondence
Suresh Mahalingam
s.mahalingam@griffith.edu.au

[1]Emerging Viruses and Inflammation Research Group, Institute for Glycomics, Griffith University, Gold Coast, QLD 4222, Australia

[2]Faculty of Applied Science, University of Canberra, Canberra, ACT 2601, Australia

[3]School of Biochemistry and Molecular Biology, The Australian National University, Canberra, ACT 0200, Australia

[4]Department of Infectious Diseases and Immunology, Sydney Medical School, University of Sydney, Sydney, NSW 2006, Australia

Alphaviruses including Barmah Forest virus (BFV) and Ross River virus (RRV) cause arthritis, arthralgia and myalgia in humans. The rheumatic symptoms in human BFV infection are very similar to those of RRV. Although RRV disease has been studied extensively, little is known about the pathogenesis of BFV infection. We sought to establish a mouse model for BFV to facilitate our understanding of BFV infectivity, tropism and pathogenesis, and to identify key pathological and immunological mechanisms of BFV infection that may distinguish between infections with BFV and RRV. Here, to the best of our knowledge, we report the first study assessing the virulence and replication of several BFV isolates in a mouse model. We infected newborn Swiss outbred mice with BFV and established that the BFV2193 prototype was the most virulent strain. BFV2193 infection resulted in the highest mortality among all BFV variant isolates, comparable to that of RRV. In comparison with RRV, C57BL/6 mice infected with BFV showed delayed onset, moderate disease scores and early recovery of the disease. BFV replicated poorly in muscle and did not cause the severe myositis seen in RRV-infected mice. The mRNAs for the inflammatory mediators TNF-α, IL-6, CCL2 and arginase-1 were highly upregulated in RRV- but not BFV-infected muscle. To our knowledge, this is the first report of a mouse model of BFV infection, which we have used to demonstrate differences between BFV and RRV infections and to further understand disease pathogenesis. With an increasing number of BFV cases occurring annually, a better understanding of the disease mechanisms is essential for future therapeutic development.

Received 14 March 2014
Accepted 11 June 2014

INTRODUCTION

Mosquito-borne alphaviruses are human pathogens that can cause diseases ranging from a self-limited rash and fever to severe arthritis or encephalitis. Arthrogenic alphaviruses such as chikungunya virus (CHIKV), Ross River virus (RRV), o'nyong-nyong virus, Barmah Forest virus (BFV), Mayaro virus and Sindbis virus are significant public health threats due to their ability to cause outbreaks of musculoskeletal disease worldwide (Boughton *et al.*, 1988; Harley *et al.*, 2001; Gérardin *et al.*, 2008; Suhrbier & Mahalingam, 2009). BFV is classified in the genus *Alphavirus* as a sole member of a distinct serocomplex of these positive-strand RNA viruses (Calisher & Karabatsos, 1988). At the amino acid level, BFV is most closely related to RRV and Semliki Forest virus (Lee *et al.*, 1997). After RRV, BFV is the second most prevalent arbovirus disease in Australia with approximately 2000 cases reported annually, with a recent marked increase in the number of people affected (Australian National Notifiable Diseases Surveillance System, 2014). The first human cases of BFV infection were reported in 1986 (Vale *et al.*, 1986), and since that time BFV has been reported throughout mainland Australia (Australian National Notifiable Diseases Surveillance System, 2014). The clinical presentation of infection closely mimics that of RRV

†These authors contributed equally to this work.

‡Present address: Department of Genome Biology, The John Curtin School of Medical Research, The Australian National University, Canberra, ACT 0200, Australia.

One supplementary figure is available with the online version of this paper.

and involves polyarthritis, arthralgia and myalgia (Jacups *et al.*, 2008). BFV infection is milder than RRV infection, with RRV-infected patients suffering from arthralgia and myalgia for longer than the BFV-infected patients (Flexman *et al.*, 1998; Jeffery *et al.*, 2006). Rash is a prominent feature in BFV patients (Jeffery *et al.*, 2006). Due to the similarity to RRV in disease presentation, without serology testing it is possible that infection with BFV is under-reported and misdiagnosed as RRV, and vice versa (McGill, 1995).

Several mosquito species including *Culex annulirostris*, *Aedes vigilax*, *Aedes normanensis* and *Aedes notoscriptus* can transmit BFV (Jacups *et al.*, 2008). Recently, another mosquito vector, *Verrallina funereal*, distributed mainly in Indonesia, Papua New Guinea and north-eastern coastal regions of Australia, was also found to be competent for BFV transmission (Jeffery *et al.*, 2006). Ever-increasing global travel and industry increase the risk of BFV extending its geographical distribution into new continents. Similar to what has been found for RRV, sero-epidemiological studies suggest that mammals, in particular marsupials, may serve as hosts for transmission of BFV (Vale *et al.*, 1986; Aldred *et al.*, 1990).

To date, most studies on BFV infection have been sero-epidemiological. The pathogenesis of BFV infection is ill defined, with no studies reported in mice. With the increasing incidence and prevalence of BFV infection, we sought to establish a mouse model to gain a better understanding of BFV infection and disease pathogenesis and to provide a platform for therapeutic development. Both newborn Swiss outbred mice and C57BL/6 mice were found to be susceptible to BFV. We identified the BFV2193 prototype as the most virulent strain; it induced disease comparable to that of RRV in Swiss outbred mice. Interestingly, BFV2193 induced moderate disease in C57BL/6 mice, in contrast to the severe myositis and arthritis caused by RRV in these mice. In line with disease severity, histological studies suggested that, unlike RRV, BFV replicated poorly in muscle and did not cause severe myositis. This was further supported by analysis of inflammatory mediators, which found that BFV did not induce the high levels of TNF-α and IL-6 transcripts in muscle seen with RRV. We conclude that, whilst BFV is highly pathogenic and displays a tropism for many tissues, it is distinct from RRV in that it causes only moderate disease and its replication in muscle tissue is limited. This is reminiscent of infection in humans, where BFV causes a milder rheumatic disease than RRV.

RESULTS

Virulence of different BFV isolates in 1-day-old Swiss mice

We first evaluated virus infectivity in 1-day-old Swiss outbred mice. As a positive control, a separate group was also infected with RRV T48 (prototype RRV strain) at 10^3 p.f.u. Six isolates of BFV from different mosquito species and geographical sources (Table 1) were tested for virulence in 1-day-old Swiss outbred mice, with viral doses ranging from 10^1 to 10^3 p.f.u. The virulence of different isolates is shown in Table 2. RRV infection resulted in death of all mice by 5 days post-infection (p.i). With BFV2193 (prototype BFV strain), 10^3 p.f.u. induced 100 % mortality by day 5 p.i., similar to that observed for RRV. Mortality decreased to 20 and 7 % at 10^2 and 10^1 p.f.u., respectively. Isolates CS30, CS1649, 96910 and G140 were less pathogenic than BFV2193. At 10^3 p.f.u., the mortality rate with these isolates was lower than the BFV2193 prototype and ranged from 20 to 60 %. For isolates CS30, CS1649 and 96910, mortality rates remained low at all dilutions ($<$50 %), and therefore the humane end-point dose for 50 % of mice infected (HD_{50}) could only be determined as $>10^3$ p.f.u., indicating that these isolates are considerably less lethal in 1-day-old Swiss mice than the BFV2193 prototype.

Different BFV isolates produce varying disease severities in 1-day-old Swiss mice

We next examined disease outcomes after BFV infection (Fig. 1). All the isolates tested induced hind leg paresis and leg extension in Swiss mice. Mean clinical scores after infection with the isolates were lower in comparison with those for BFV2193 (Fig. 1). In agreement with the mortality studies, mice infected with the isolate CS1649 exhibited much reduced disease severity, whilst the BFV2193 infection caused death in all mice. Interestingly, despite having HD_{50} values above 1000, CS30 and 96910 did not appear to show reduced disease scores in comparison with Murweh and G140, suggesting that these viruses are as capable of causing severe disease symptoms in mice but without lethality.

BFV prototype tissue tropism in 1-day-old Swiss outbred mice

BFV tissue tropism was investigated using the BFV prototype strain BFV2193. To identify sites of virus replication, viral titres in blood, muscle and brain tissue were determined in infected mice. As shown in Fig. 2, viral titres were relatively high in blood within the first 2 days but dropped sharply from day 3 onwards. By day 6, virus was not detectable in the blood. In contrast, virus was still detectable at days 8 and 9 in muscle and brain. Viral titres were very high from days 1 to 5, with similar kinetics in muscle and brain. Thus, BFV showed tissue tropism to blood, muscle and brain in 1-day-old Swiss mice. However, clearance of virus was much faster in blood than in muscle or brain.

BFV does not induce severe musculoskeletal disease in C57BL/6 mice

In mouse models of related alphaviruses (RRV and CHIKV), infection results in arthritis and myositis in mice (Lidbury *et al.*, 2000; Morrison *et al.*, 2006; Gardner *et al.*, 2010). To assess the ability of BFV to induce arthritis and

Table 1. Isolates of BFV from *C. annulirostris* and *A. vigilax* mosquitoes from various locations in Australia

Virus	Vector source	Area isolated	Year	Reference
BFV2193	*C. annulirostris*	Murray Valley, VIC	1974	Marshall *et al.* (1982)
Murweh	*C. annulirostris*	Charlesville, QLD	1974	Doherty *et al.* (1979)
G140	*A. vigilax*	Gippsland Lakes, VIC	1989	Aldred *et al.* (1990)
96910	*A. vigilax*	Mogo, NSW	1985	Vale *et al.* (1986)
CS30	*C. annulirostris*	Beatrice Hill, NT	1975	Standfast *et al.* (1984)
CS1649	*C. annulirostris*	Peachester, QLD	1984	Standfast *et al.* (1984)

myositis, we analysed BFV infection in parallel with the established C57BL/6 mouse model of RRV-induced myositis and arthritis (Morrison *et al.*, 2006). In BFV-infected mice, signs were mild, including a hunched posture with lethargy and ruffled fur (with a maximum clinical score of 2). Mice infected with BFV did not display the arthritic signs routinely observed in RRV-infected mice, with only a few mice developing slight hind-limb weakness. In contrast, RRV-infected mice developed severe hind-limb paralysis and dysfunction (Fig. 3a). In addition to the moderate disease scores at the peak of disease, BFV-infected mice also had delayed disease onset (day 4 in RRV vs day 6/7 in BFV) and early recovery from disease symptoms (day 15 in BFV vs day 18 in RRV). Infection with RRV resulted in a severe reduction in normal weight gain to the point of weight loss during peak disease (Fig. 3b). In contrast, BFV-infected mice showed a moderate reduction in weight gain compared with mock-infected controls (significant from day 3 to day 18 p.i., $P<0.001$) and a significantly higher level of weight gain than RRV-infected mice (significant from day 6 to day 18 p.i., $P<0.001$). BFV-infected mice did not show any weight loss over the course of the experiment (Fig. 3b).

Tissue tropism and spread of BFV in C57BL/6 mice is distinct from RRV

In C57BL/6 mice, RRV infection targets bone, joint and skeletal muscle (Morrison *et al.*, 2006). To determine the tissue tropism of BFV, we infected C57BL/6 mice and analysed their blood, ankles and quadriceps for the presence of virus. BFV titres rose from the time of infection, peaking at day 3 p.i. in serum, ankle joints and muscle tissue (Fig. 4). Similar to RRV, BFV infection of C57BL/6 mice resulted in high levels of viraemia and extensive virus replication in the ankle tissues (Fig. 4a, b). Unlike RRV, BFV did not replicate to high levels in the muscle tissue (Fig. 4c): BFV was only detectable at days 3 and 5 p.i. and was below the limit of detection at day 1 p.i. (despite high titres detected in serum and ankle joints) and day 10 p.i. (despite moderate titres detectable in the ankle

Table 2. Mortality induced by different BFV strains in one-day-old Swiss mice

One-day-old mice were inoculated subcutaneously with one of six BFV isolates and observed for mortality and morbidity. Mock-infected controls were injected with 30 µl PBS. Data represent the mean of three individual experiments. MTD, mean time to humane end point, measured in days; CD_{50}, 50 %: clinical dose (dose that caused symptoms in 50 % of the mice; range of symptoms considered positive were: mild leg stiffness, through to hind leg paralysis, significant weight loss and death); HD_{50}, humane end-point dose for 50 % of mice infected.

Isolate	Dose (p.f.u.)	Mortality (%)	MTD (± SD)	HD_{50}
Mock	0	0	–	–
RRV (T48) prototype	1000	100	5±0	–
BFV2193 prototype	1000	100	5.3±2.6	
	100	22.2	5.0±2.8	90
	10	7.2	10.5±2.1	
Murweh	1000	64	4.6±3.6	
	10	19	9	210
G140	1000	65	8.8±3.5	
	10	27.3	8.0±1.0	250
96910	1000	19.2	10±5.6	
	10	21.7	8.0±4.3	>1000
CS30	1000	34.8	7.0±7.7	
	10	8.7	3.0	>1000
CS1649	1000	20.7	10.8±3.3	
	10	15.4	16.8±5.3	>1000

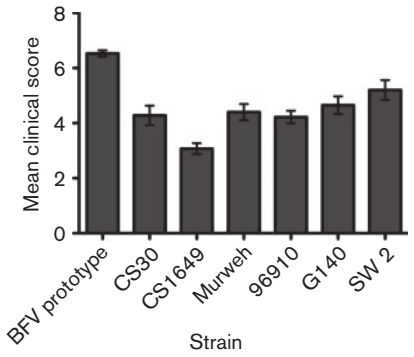

Fig. 1. Mean peak clinical scores of 1-day-old Swiss mice infected with different BFV isolates. One-day-old Swiss mice were infected subcutaneously with 10^3 p.f.u. of the specified isolate or were mock infected with diluent alone. Mice were monitored daily and scored for signs of disease based on the following scale: 1, healthy; 2, slight hind leg stiffness; 3, pronounced hind leg stiffness/paresis; 4, hind leg paresis and leg extension; 5, significant weight loss and hind leg paresis; 6, death after day 5 p.i; 7, death during days 1–5 p.i. Each data point represents the mean of peak disease observed ± SEM of mice in groups of 11–36.

joints). This contrasted with RRV infection (Fig. 4c), which replicates well in all tissues, particularly in quadriceps (Morrison *et al.*, 2006, 2007, 2008; Lidbury *et al.*, 2008; Herrero *et al.*, 2011). These results show that BFV produces a systemic infection in C57BL/6 mice and replicates effectively in joint tissues, whilst its replication in muscle tissues is limited. To confirm whether this was a mouse-specific phenomenon, cell lines for human muscle (rhabdomyosarcoma) and epithelial (HeLa) cells were infected with BFV and compared with Vero cells *in vitro*. BFV replicated efficiently in Vero cells but showed slower growth in rhabdomyosarcoma (RD) cells, suggesting a reduced tropism for muscle cells (Fig. S1, available in the online Supplementary Material).

BFV induces moderate inflammation in C57BL/6 mice

Previously, we showed that peak disease in RRV-infected C57BL/6 mice corresponded with severe inflammation of the quadriceps muscle and ankle joints (Morrison *et al.*, 2006). To determine whether the reduction in disease severity in BFV-infected C57BL/6 mice corresponded to a reduction in inflammation, C57BL/6 mice were infected with 10^3 p.f.u. BFV or RRV. Mice were sacrificed on day 10 p.i. (peak disease), and quadriceps muscle and ankle tissues were collected for histological analysis. Histological analysis of quadriceps muscle stained with haematoxylin and eosin showed a reduced level of immune filtrates compared with the extensive myositis observed in RRV-infected mice (Fig. 5a). The ankle joints from BFV-infected mice showed an increase in inflammatory infiltration in the connective tissue surrounding the joints, similar to that observed in RRV-infected mice (Fig. 5b).

BFV infection induces pro-inflammatory cytokines

In light of the moderate disease outcome of BFV infection, we sought to characterize the inflammatory profile in the quadriceps and ankle, to correlate it with the tissue pathology and compare it with RRV infection. The transcripts of inflammatory cytokines TNF-α, IFN-γ, IL-1β and IL-6, and the chemokines CCL2 (MCP-1), CXCL1 (KC, murine IL-8 homologue) and other pro-inflammatory proteins S100A8, S100A9 and arginase 1 were examined. As shown in Fig. 6(a), whilst BFV infection induced a significant elevation of TNF-α, IFN-γ, IL-1β and IL-6 in quadriceps, RRV was much more potent in inducing TNF-α, IL-1-β and IL-6. In contrast, there was no significant difference between BFV and RRV infections in the TNF-α, IL-1β and IL-6 transcripts in the ankle. Similarly, arginase 1 was elevated in both RRV- and BFV-infected mice; however, it was only in quadriceps that RRV-infected mice showed a much greater

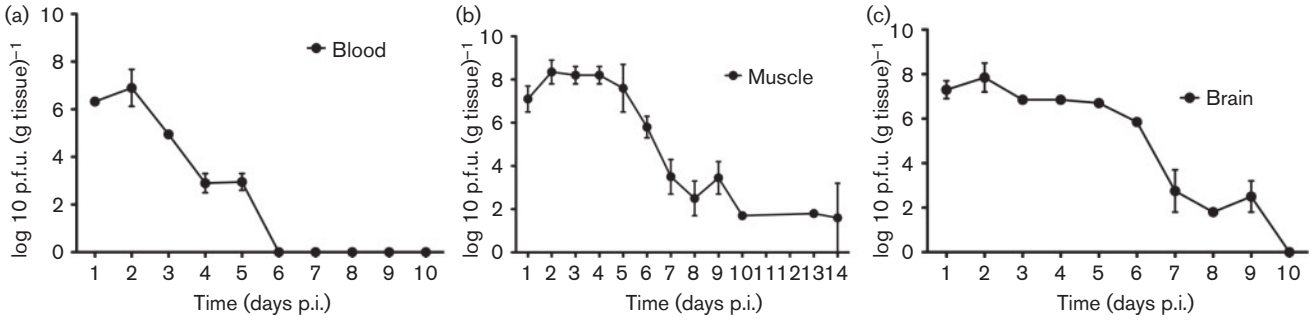

Fig. 2. BFV prototype titres in the blood, muscle and brain of 1-day-old Swiss outbred mice. One-day-old Swiss mice were infected subcutaneously with 10^1 p.f.u. of the prototype BFV strain. Blood (a), muscle (b) and brain tissues (c) were isolated on the indicated days, homogenized and the amount of infectious virus was determined by plaque assay on Vero cells. Each data point represents the mean ± SEM of at least three mice. The limit of detection was standardized at 10^2 p.f.u. ml^{-1} for serum and 10^2 p.f.u. g^{-1} for tissue.

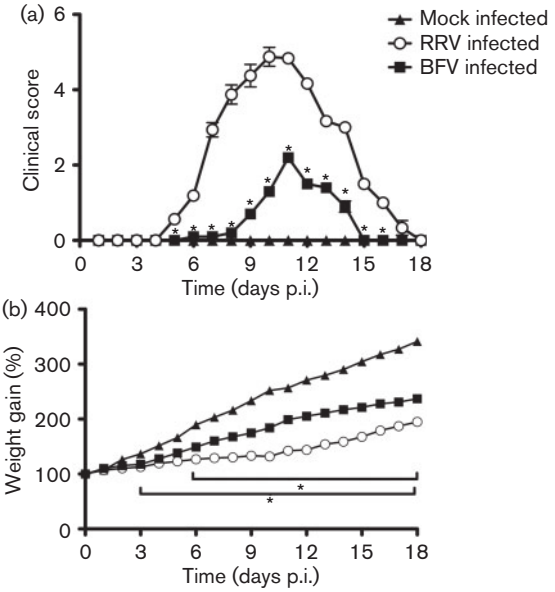

Fig. 3. BFV induces mild disease in C57BL/6 mice. Twenty-one-day-old C57BL/6 mice were infected subcutaneously with 10^3 p.f.u. BFV or 10^3 p.f.u. RRV or were mock infected with diluent alone. (a) Mice were scored for the development of hind-limb dysfunction and disease based on the following scale: 0, no disease signs; 1, ruffled fur; 2, very mild hind limb weakness; 3, mild hind limb weakness; 4, moderate hind limb weakness and dragging of hind limbs; 5, severe hind limb weakness/dragging; 6, complete loss of hind limb function; 7, moribund; and 8, death. Each data point represents the mean ± SEM of 5–10 mice and is representative of four independent experiments. *$P<0.05$ using a Mann–Whitney test. (b) Mouse weight was monitored at 24 h intervals. Mock-infected mice were scored zero for the duration of the experiment (data not shown). Each data point represents the mean ± SEM of 5–10 mice and is representative of three independent experiments. *$P<0.05$ compared with mock-infected controls using two-way ANOVA with a Bonferroni post-test.

level of arginase 1 than in mice infected with BFV (Fig. 6b). This is in line with the histological analysis (Fig. 5), in which RRV caused a higher level of cell infiltrates and tissue damage in quadriceps but not in ankle. Indeed, S100A8 and S100A9 transcripts in quadriceps were highly upregulated only in RRV-infected mouse suggesting the presence of active inflammation (Fig. 6c). Above all, CCL2 and CXCL1 consistently showed a dramatic increase in both quadriceps and ankle of RRV-infected mice in contrast to BFV-infected mice (Fig. 6d). CCL2 has been shown to play an important role in enhancing RRV disease severity (Rulli *et al.*, 2009). Additionally, in both RRV- and BFV-infected quadriceps and ankles, IFN-γ was also highly upregulated.

DISCUSSION

Among the alphaviruses circulating in Australia, BFV is the second most common mosquito-borne virus after RRV. The recent rise in the number of BFV infections is a cause for concern. In 2005–2006, there were 1895 notifications of BFV infections in Queensland, Australia. Clinically, BFV causes rheumatic disease symptoms very similar to RRV (Jacups *et al.*, 2008). Due to the absence of an animal model of BFV infection, our understanding of BFV disease pathogenesis is limited. However, recent advances in studying the pathogenesis of related alphaviruses such as RRV and CHIKV provide a framework for probing BFV pathogenesis. We sought to establish a mouse model for BFV to facilitate our understanding of BFV infectivity, tropism and pathogenesis. Furthermore, we attempted to identify the key pathological and immunological mechanisms of BFV infection, in comparison with the established RRV model, to address whether such mechanisms correlate with the observation in humans.

Our initial studies with Swiss outbred mice indicated that BFV is pathogenic in mice and spreads rapidly to brain and muscle. The virulence varied among isolates when mortality was measured, with the results suggesting a difference in infectivity in relation to dose among different strains. Although CS1649, CS30 and 96910 were much less lethal to mice, 10^3 p.f.u. CS30 and 96910 induced disease symptoms that were more severe than CS1649 and were virtually the same as Murweh and G140. This indicates that, whilst disease symptoms and mortality may both be indicators of viral virulence, these two parameters do not necessarily correlate, and it is likely that the IFN response is an additional factor contributing to virus-induced mortality. In this regard, we routinely see RRV induce earlier morbidity and higher rates of mortality at lower infection (p.f.u. per mouse) doses (Lidbury *et al.*, 2011). Similar observations were seen in herpes simplex virus type 1 (HSV-1) infection of mice where IFN induced after injection with a high dose of HSV-1 protects mice, whilst injection with low doses of virus resulted in mortality due to a low-level IFN response at the site of infection (Zawatzky *et al.*, 1982). Based on the virulence study, the BFV2193 prototype was considered to be the most virulent strain as it caused high mortality with a low mean time to death and a low HD_{50} in newborn Swiss mice.

Based on our experience with RRV, we infected C57BL/6 mice with the BFV2193 prototype to develop an animal model for BFV. Disease signs were mild in BFV-infected C57BL/6 mice and included lethargy, hunched posture and ruffled fur with very mild hind limb dysfunction in only a small number of mice (contrasting with the more severe disease in RRV-infected C57BL/6 mice). The lack of muscle destruction and absence of hind-leg weakness in BFV-infected mice was consistent with the low virus titres recovered from quadriceps muscle, indicative of low levels of replication. This contrasted to RRV-infected mice, which showed severe rheumatic symptoms including hind-limb weakness and dragging accompanied by higher levels of virus replication in quadriceps muscle (Morrison *et al.*, 2006). Similar to RRV, previous studies on the related alphaviruses CHIKV and Mayaro have shown a high level

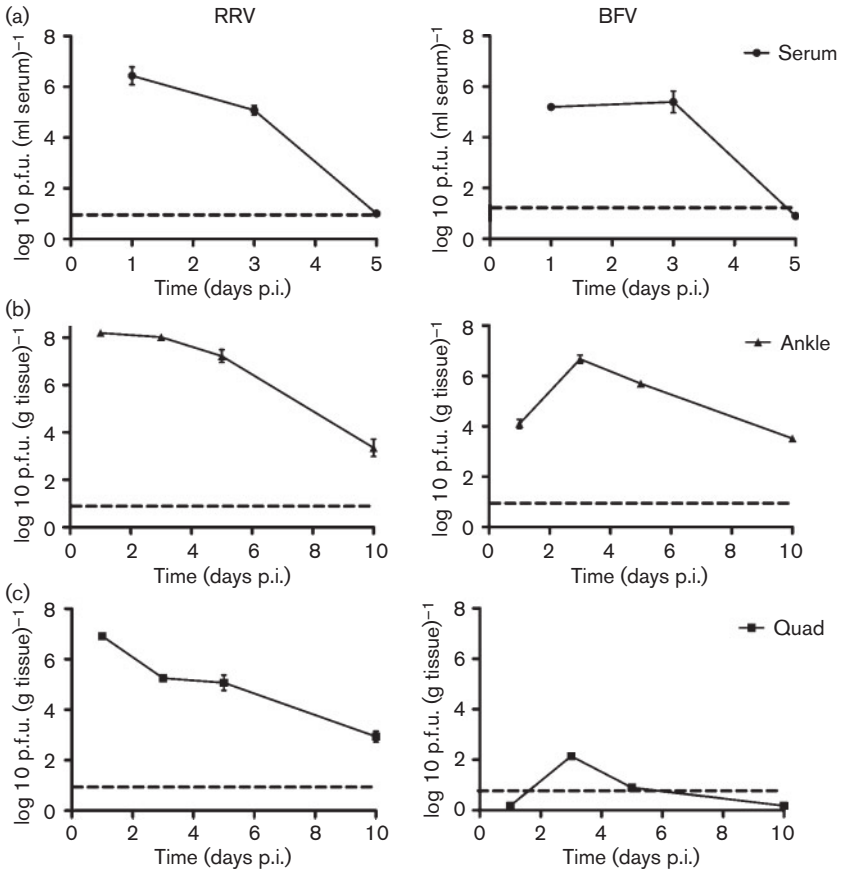

Fig. 4. BFV tissue titres in C57BL/6 mice. Twenty-one-day-old C57BL/6 mice were infected subcutaneously with 10^3 p.f.u. BFV or 10^3 p.f.u. RRV. At days 1, 3, 5 and 10 p.i. the serum (a), ankle (b) and quadriceps (Quad; c) tissues were harvested and homogenized and the amount of infectious virus determined by plaque assay on Vero cells. Each data point represents the mean ± SEM of five mice. The limit of detection is indicated by the dashed line.

of virus replication in muscle tissues (Gardiner *et al.*, 1990; Ziegler *et al.*, 2008). In particular, a recent study has shown that the CHIKV strain LR2006OPY1 causes greater disease severity in C57BL/6 mice corresponding to high muscle tropism compared with the CHIKV strain 37997, demonstrating the correlation between viral burden in skeletal tissue and disease (Rohatgi *et al.*, 2014). Overall, BFV differs from these viruses in having reduced tropism for muscle tissue. Of relevance to the present study is our preliminary observation that BFV replicated poorly in both human muscle cell lines (Fig. S1) and primary human myoblast compared with RRV (J. Johal and S. Mahalingam, unpublished data). BFV persisted longer in the muscle tissue of newborn Swiss mice than 21-day-old C57BL/6 mice. The lower immune competence of the younger mice is a probable explanation for this, as has been reported for a number of viruses (Reinarz *et al.*, 1971; Ryman *et al.*, 2007).

The kinetics of disease scores were very similar between RRV- and BFV-infected mice in that they required a similar time to reach the peak of the disease, although BFV infection appeared to have a slower disease onset, faster recovery and milder inflammation. Such coordination suggests that both diseases follow a similar course of immune activation and resolution and that RRV is more pathogenic than BFV in the C57BL/6 model. Indeed, at the peak of disease, histological and cytokine transcriptional analyses suggested that the immunopathogenicity of BFV was weaker than that of RRV. BFV-infected mice showed moderate immune infiltration in the quadriceps at the peak of disease, although their ankles demonstrated comparable infiltration to RRV-infected mice. This observation was consistent with the analysis of inflammatory mediators, which demonstrated particularly heightened TNF-α, IL-6 and arginase 1 in RRV- but not BFV-infected quadriceps. Additionally, RRV was capable of inducing high levels of S100A8 and S100A9 in quadriceps in contrast to BFV. In line with this, the pro-inflammatory role for S100A8 and S100A9 has been implicated in various acute and chronic inflammatory disease models (Gebhardt *et al.*, 2006) and therefore may explain the worsened muscle inflammation in RRV infection. CCL2 was also upregulated in both RRV- and BFV-infected mice, with a significantly higher level in RRV infection. CCL2 is a key regulator of leukocyte recruitment that has been shown previously to contribute to disease severity in the mouse model of RRV (Deshmane *et al.*, 2009; Rulli *et al.*, 2009). RRV-infected ankle tissue did not exhibit a greater level of immune infiltration than BFV, which may be due to the similar ankle joint tropism of the two viruses, with both replicating to high titres in the ankle joint (Fig. 4) and primary bone cells derived from human joints (A. Choo & S. Mahalingam, unpublished data).

In this study, to the best of our knowledge, we have demonstrated for the first time the pathogenicity of BFV in

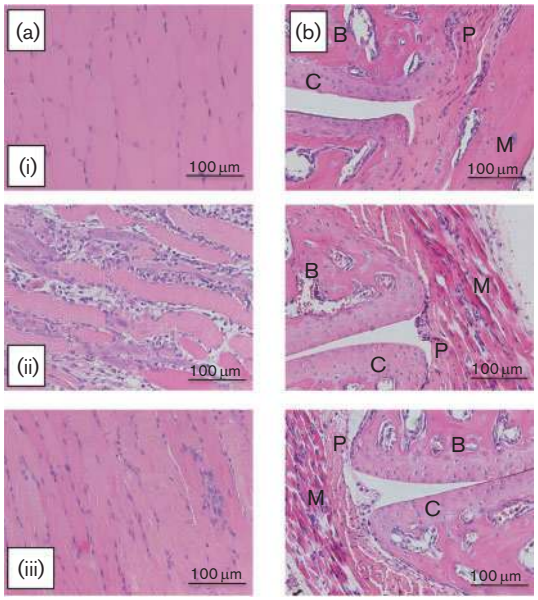

Fig. 5. BFV induces moderate inflammation in C57BL/6 mice. Twenty-one-day-old C57BL/6 mice were infected subcutaneously with 10^3 p.f.u. BFV or 10^3 p.f.u. RRV or were mock infected with diluent alone. At 10 days p.i., mice were sacrificed and perfused with 4 % paraformaldehyde. Quadriceps (a) and ankle tissues (b) were removed and paraffin embedded and 5 µm sections were generated. Sections were stained with haematoxylin and eosin. The panels show mock-infected (i), RRV-infected (ii) and BFV-infected (iii) tissues. Images are representative of at least five mice per group. Magnification ×200. B, bone; C, cartilage; P, periosteum; M, muscle.

inbred and outbred mice. In contrast to RRV, BFV infection of adult mice did not induce severe myositis. The disease kinetics and cytokine profiles in C57BL/6 mice indicated that BFV infection is similar to RRV infection but follows a milder course. As many inflammatory mediators such as cytokines and chemokines, as well as effector cells like macrophages, have been shown to play important roles in RRV infection, the inflammatory profile of BFV infection will be thoroughly examined in future studies. This study describes a new mouse model of BFV infection, which shares key pathogenic events with the related arthritogenic alphavirus RRV, but also differs from RRV in several important aspects. The model is likely to contribute to an increased understanding of the pathogenesis of BFV-induced disease and will have a direct impact on human health through the development of improved therapeutics. Translation of this model to the emerging human disease will be an important step in understanding viral arthritis.

METHODS

Viruses and cells. The BFV isolates used in the study were isolated from *C. annulirostris* and *A. vigilax* mosquitoes from various locations in Australia (Table 1). The passage history of these isolates is the same as described for BF2193 (GenBank accession no. U73745.1) by Lee et al. (1997). Briefly, initial propagation was performed in suckling mouse brain, followed by *in vitro* expansion in Vero (ATCC CCL-81) or BHK (ATCC CCL-10) cells. Working virus stocks for experiments were grown in BHK cells and no working stock exceeded three passages in Vero or BHK cells. The prototype RRV (T48 strain; kindly provided by Richard Kuhn, Purdue University, IN, USA; GenBank accession number GQ433359) was used as a comparison throughout the study. The RRV-T48 strain was originally isolated in Queensland, Australia from *A. vigilax* mosquitoes (Doherty *et al.*, 1979). Viruses were propagated using Vero cells, which were cultured in OptiMEM (Invitrogen) medium containing 3 % heat-inactivated newborn calf serum (HI-NBS; Sigma-Aldrich) and 2 % penicillin/streptomycin/neomycin. *In vitro* replication studies were performed in Vero, RD (ATCC CCL-136) and HeLa (ATCC CCL-2) cell lines infected at an m.o.i. of 1. Immunofluorescence (IF) was performed by fixing cells in acetone : methanol (1 : 1) and staining with a primary mouse anti-BFV E2 mAb (clone 9E8; Tropbio) and a secondary Alexa Fluor 488-conjugated donkey anti-mouse antibody (Molecular Probes). Slides were mounted with SlowFade Gold with DAPI (Molecular Probes) before being viewed with an Olympus BX51 fluorescence microscope. All viral titrations were performed by plaque assay as described previously (Lidbury & Mahalingam, 2000). Partial sequences of the BFV strains used in this study have been published previously (Poidinger *et al.*, 1997). A high degree of sequence identity (98–100 %) was found between the BFV isolates (Poidinger *et al.*, 1997).

Mice. Pregnant Swiss outbred mice were obtained from the John Curtin School of Medical Research, Canberra, Australia. Female inbred 21-day-old C57BL/6 mice were obtained from the Animal Resource Centre, Perth, Australia.

For infection of 1-day-old mice, dilutions in PBS of 10^3 to 10^1 p.f.u. BFV or 10^3 p.f.u. RRV were made up in a final volume of 30 µl. For infection of 21-day-old C57BL/6 mice, 10^3 p.f.u. BFV or 10^3 p.f.u. RRV were diluted in PBS in a final volume of 50 µl. Mock-infected mice received diluent alone. All injections were administered subcutaneously in the thorax. For assessment of clinical disease, mice were weighed and scored for clinical signs every 24 h for the duration of the experiment. For infection of 1-day-old Swiss mice, clinical scores were based on the following scale: 1, healthy; 2, slight hind-leg stiffness (mouse can still walk and uses all four legs but is imbalanced); 3, pronounced hind-leg stiffness/paresis (mouse starts dragging hind limbs); 4, hind-leg paresis and leg extension (legs are fully extended behind the mouse and 100 % immobile); 5, significant weight loss (defined as weight being at least three SDs below the mean weight observed in the mock-infected control group) and hind-leg paresis; 6, death after day 5 p.i; and 7, death prior to day 5 p.i. For infection in 21-day old C57BL/6 mice, clinical scores were assessed based on the development of hind-limb dysfunction and disease and were scored as follows: 0, no disease signs; 1, ruffled fur; 2, lethargy and hunched posture; 3, very mild hind-limb weakness; 4, mild to moderate hind-limb weakness; 5, severe hind-limb weakness/dragging; 6, complete loss of hind-limb function; 7, moribund; and 8, death.

To determine the viral titres in tissues, mice were sacrificed by CO_2 asphyxiation and perfused with PBS. Tissues from brain, spleen, ankle and quadriceps muscle were removed, weighed and homogenized in PBS supplemented with 1 % HI-NBS. Viral titres were determined by plaque assay on Vero cells as described previously (Lidbury & Mahalingam, 2000).

Histology. Mice were sacrificed and perfused with 4 % paraformldehyde. Tissues were collected, fixed in 4 % paraformldehyde, ankles decalcified and embedded in paraffin sections. Sections (5 µM) were prepared and stained with haematoxylin and eosin.

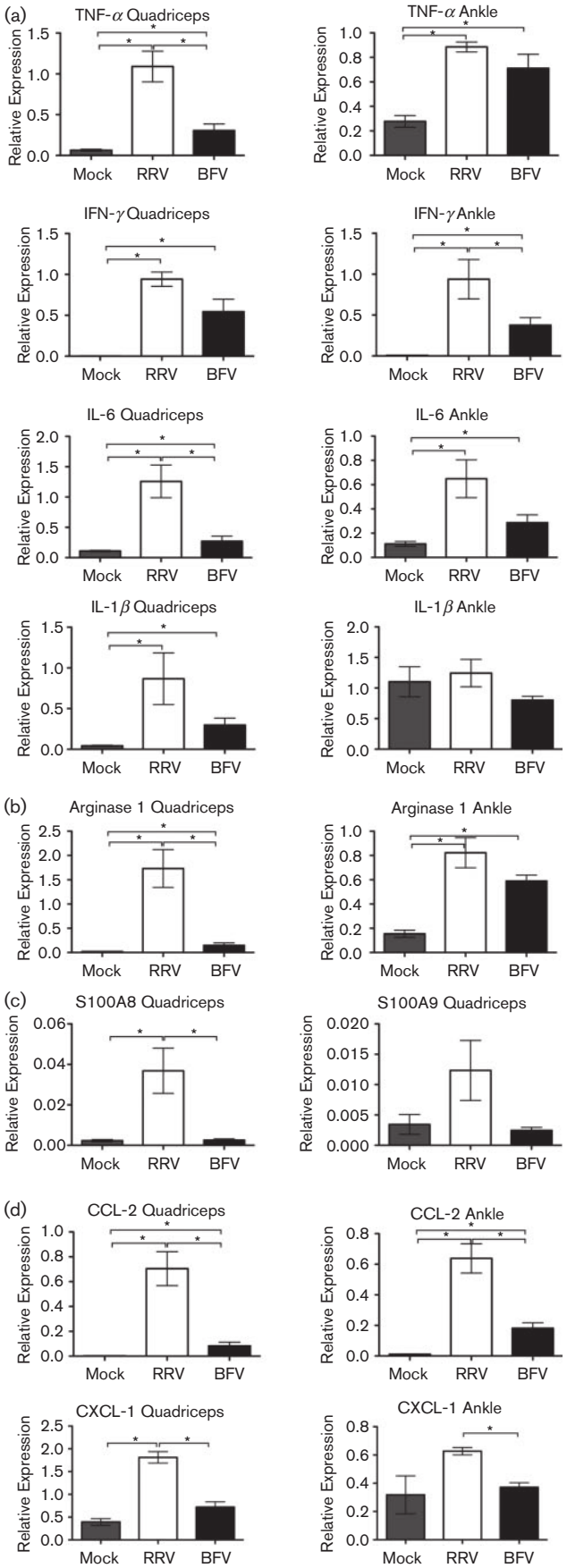

Fig. 6. BFV induces the expression of inflammatory mediators in C57BL/6 mice. Twenty-one-day old C57BL/6 mice were infected subcutaneously with 10^3 p.f.u. BFV (filled bars), 10^3 p.f.u. RRV (open bars) or mock-infected with diluent alone (shaded bars). Total RNA from quadriceps muscle and ankle joint tissues was isolated at 10 days p.i. and analysed for mRNA expression by quantitative reverse transcriptase-PCR of TNF-α, IFN-γ, IL-6 and IL-1β (a), arginase 1 (b), S100A8 and S100A9 (c) and CCL2 and CXCL-1 (d). Data were normalized to the housekeeping gene hypoxanthine phosphoribosyltransferase 1 (*HPRT1*) and expressed as relative expression. *$P<0.05$ using Student's *t*-test. Each bar represents the mean ± SEM for five mice.

Real-time PCR. Total RNA was isolated with TriReagent (Ambion) according to the manufacturer's instructions. RNA was reverse transcribed with random primers (Promega) and cDNA was generated with mouse murine leukemia virus reverse transcriptase (Invitrogen). SYBR Green real-time PCR was performed using a total of 1 µg template cDNA and commercially available QuantiTec primers for CCL2, CXCL1, TNF-α, IFN-γ, IL-1β, IL-6, arginase 1, S100A9 and S100A8 (Qiagen) with FastStart SYBR-Green Master (Roche) on a CFX96 Touch Real-Time PCR System. The real-time PCR data were calculated using the comparative threshold cycle method and the iCycler CFX96 analyser software (Bio-Rad).

Statistical analysis. Real-time PCR data were evaluated statistically by unpaired *t*-tests. Weights were analysed using two-way ANOVA with a Bonferroni post-test. All data were tested for normality using the D'Agostino–Pearson normality test prior to analysis with these parametric tests. Clinical scores were analysed using the non-parametric Mann–Whitney test. Statistics were performed with GraphPad Prism 5.02.

ACKNOWLEDGEMENTS

We thank Drs Lyn Dalgarno, Ron Weir and Eva Lee (all from the Australian National University) for early support of the BFV study. S. M. is the recipient of an Australian NHMRC Senior Research Fellowship. The authors gratefully acknowledge the critical reading and expert advice provided by Dr Linda Hueston (Westmead Hospital, Sydney, Australia); we also acknowledge Mr Glynn Rees and the Queensland Institute for Medical Research Histochemistry Laboratory for immunohistochemical staining. This project was supported by funding from the Australian National Health and Medical Research Council to S. M. (grant ID 508600).

REFERENCES

Aldred, J., Campbell, J., Davis, G., Lehmann, N. & Wolstenholme, J. (1990). Barmah Forest virus in the Gippsland Lakes region, Victoria. *Med J Aust* **153**, 434.

Australian National Notifiable Diseases Surveillance System (2014). Australian Department of Health National Notifiable Diseases Surveillance System. http://www9.health.gov.au/cda/source/cda-index.cfm

Boughton, C. R., Hawkes, R. A. & Naim, H. M. (1988). Illness caused by a Barmah Forest-like virus in New South Wales. *Med J Aust* **148**, 146–147.

Calisher, C. & Karabatsos, N. (1988). *Arbovirus Serogroups: Definition and Geographic Distribution.* Boca Raton, FL: CRC Press.

Deshmane, S. L., Kremlev, S., Amini, S. & Sawaya, B. E. (2009). Monocyte chemoattractant protein-1 (MCP-1): an overview. *J Interferon Cytokine Res* **29**, 313–326.

Doherty, R. L., Carley, J. G., Kay, B. H., Filippich, C., Marks, E. N. & Frazier, C. L. (1979). Isolation of virus strains from mosquitoes collected in Queensland, 1972–1976. *Aust J Exp Biol Med Sci* **57**, 509–520.

Flexman, J. P., Smith, D. W., Mackenzie, J. S., Fraser, J. R., Bass, S. P., Hueston, L., Lindsay, M. D. & Cunningham, A. L. (1998). A comparison of the diseases caused by Ross River virus and Barmah Forest virus. *Med J Aust* **169**, 159–163.

Gardiner, S. M., Compton, A. M., Bennett, T., Domin, J. & Bloom, S. R. (1990). Regional hemodynamic effects of neuromedin U in conscious rats. *Am J Physiol* **258**, R32–R38.

Gardner, J., Anraku, I., Le, T. T., Larcher, T., Major, L., Roques, P., Schroder, W. A., Higgs, S. & Suhrbier, A. (2010). Chikungunya virus arthritis in adult wild-type mice. *J Virol* **84**, 8021–8032.

Gebhardt, C., Németh, J., Angel, P. & Hess, J. (2006). S100A8 and S100A9 in inflammation and cancer. *Biochem Pharmacol* **72**, 1622–1631.

Gérardin, P., Guernier, V., Perrau, J., Fianu, A., Le Roux, K., Grivard, P., Michault, A., de Lamballerie, X., Flahault, A. & Favier, F. (2008). Estimating Chikungunya prevalence in La Réunion Island outbreak by serosurveys: two methods for two critical times of the epidemic. *BMC Infect Dis* **8**, 99.

Harley, D., Sleigh, A. & Ritchie, S. (2001). Ross River virus transmission, infection, and disease: a cross-disciplinary review. *Clin Microbiol Rev* **14**, 909–932.

Herrero, L. J., Nelson, M., Srikiatkhachorn, A., Gu, R., Anantapreecha, S., Fingerle-Rowson, G., Bucala, R., Morand, E., Santos, L. L. & Mahalingam, S. (2011). Critical role for macrophage migration inhibitory factor (MIF) in Ross River virus-induced arthritis and myositis. *Proc Natl Acad Sci U S A* **108**, 12048–12053.

Jacups, S. P., Whelan, P. I. & Currie, B. J. (2008). Ross River virus and Barmah Forest virus infections: a review of history, ecology, and predictive models, with implications for tropical northern Australia. *Vector Borne Zoonotic Dis* **8**, 283–298.

Jeffery, J. A., Kay, B. H. & Ryan, P. A. (2006). Role of *Verrallina funerea* (Diptera: Culicidae) in transmission of Barmah Forest virus and Ross River virus in coastal areas of eastern Australia. *J Med Entomol* **43**, 1239–1247.

Lee, E., Stocks, C., Lobigs, P., Hislop, A., Straub, J., Marshall, I., Weir, R. & Dalgarno, L. (1997). Nucleotide sequence of the Barmah Forest virus genome. *Virology* **227**, 509–514.

Lidbury, B. A. & Mahalingam, S. (2000). Specific ablation of antiviral gene expression in macrophages by antibody-dependent enhancement of Ross River virus infection. *J Virol* **74**, 8376–8381.

Lidbury, B. A., Simeonovic, C., Maxwell, G. E., Marshall, I. D. & Hapel, A. J. (2000). Macrophage-induced muscle pathology results in morbidity and mortality for Ross River virus-infected mice. *J Infect Dis* **181**, 27–34.

Lidbury, B. A., Rulli, N. E., Suhrbier, A., Smith, P. N., McColl, S. R., Cunningham, A. L., Tarkowski, A., van Rooijen, N., Fraser, R. J. & Mahalingam, S. (2008). Macrophage-derived proinflammatory factors contribute to the development of arthritis and myositis after infection with an arthrogenic alphavirus. *J Infect Dis* **197**, 1585–1593.

Lidbury, B. A., Rulli, N. E., Musso, C. M., Cossetto, S. B., Zaid, A., Suhrbier, A., Rothenfluh, H. S., Rolph, M. S. & Mahalingam, S. (2011). Identification and characterization of a ross river virus variant that grows persistently in macrophages, shows altered disease kinetics in a mouse model, and exhibits resistance to type I interferon. *J Virol* **85**, 5651–5663.

Marshall, I. D., Thibos, E. & Clarke, K. (1982). Species composition of mosquitoes collected in the Murray Valley of South-eastern Australia during an epidemic of arboviral encephalitis. *Aust J Exp Biol Med Sci* **60**, 447–456.

McGill, P. E. (1995). Viral infections: α-viral arthropathy. *Baillieres Clin Rheumatol* **9**, 145–150.

Morrison, T. E., Whitmore, A. C., Shabman, R. S., Lidbury, B. A., Mahalingam, S. & Heise, M. T. (2006). Characterization of Ross River virus tropism and virus-induced inflammation in a mouse model of viral arthritis and myositis. *J Virol* **80**, 737–749.

Morrison, T. E., Fraser, R. J., Smith, P. N., Mahalingam, S. & Heise, M. T. (2007). Complement contributes to inflammatory tissue destruction in a mouse model of Ross River virus-induced disease. *J Virol* **81**, 5132–5143.

Morrison, T. E., Simmons, J. D. & Heise, M. T. (2008). Complement receptor 3 promotes severe ross river virus-induced disease. *J Virol* **82**, 11263–11272.

Poidinger, M., Roy, S., Hall, R. A., Turley, P. J., Scherret, J. H., Lindsay, M. D., Broom, A. K. & Mackenzie, J. S. (1997). Genetic stability among temporally and geographically diverse isolates of Barmah Forest virus. *Am J Trop Med Hyg* **57**, 230–234.

Reinarz, A. B. G., Broome, M. G. & Sagik, B. P. (1971). Age-dependent resistance of mice to Sindbis virus infection: viral replication as a function of host age. *Infect Immun* **3**, 268–273.

Rohatgi, A., Corbo, J. C., Monte, K., Higgs, S., Vanlandingham, D. L., Kardon, G., Lenschow, D. J. & Perlman, S. (2014). Infection of myofibers contributes to increased pathogenicity during infection with an epidemic strain of chikungunya virus. *J Virol* **88**, 2414–2425.

Rulli, N. E., Guglielmotti, A., Mangano, G., Rolph, M. S., Apicella, C., Zaid, A., Suhrbier, A. & Mahalingam, S. (2009). Amelioration of alphavirus-induced arthritis and myositis in a mouse model by treatment with bindarit, an inhibitor of monocyte chemotactic proteins. *Arthritis Rheum* **60**, 2513–2523.

Ryman, K. D., Gardner, C. L., Meier, K. C., Biron, C. A., Johnston, R. E. & Klimstra, W. B. (2007). Early restriction of alphavirus replication and dissemination contributes to age-dependent attenuation of systemic hyperinflammatory disease. *J Gen Virol* **88**, 518–529.

Standfast, H. A., Dyce, A. L., St George, T. D., Muller, M. J., Doherty, R. L., Carley, J. G. & Filippich, C. (1984). Isolation of arboviruses from insects collected at Beatrice Hill, Northern Territory of Australia, 1974-1976. *Aust J Biol Sci* **37**, 351–366.

Suhrbier, A. & Mahalingam, S. (2009). The immunobiology of viral arthritides. *Pharmacol Ther* **124**, 301–308.

Vale, T. G., Carter, I. W., McPhie, K. A., James, G. S. & Cloonan, M. J. (1986). Human arbovirus infections along the south coast of New South Wales. *Aust J Exp Biol Med Sci* **64**, 307–309.

Zawatzky, R., Gresser, I., DeMaeyer, E. & Kirchner, H. (1982). The role of interferon in the resistance of C57BL/6 mice to various doses of herpes simplex virus type 1. *J Infect Dis* **146**, 405–410.

Ziegler, S. A., Lu, L., da Rosa, A. P., Xiao, S. Y. & Tesh, R. B. (2008). An animal model for studying the pathogenesis of chikungunya virus infection. *Am J Trop Med Hyg* **79**, 133–139.